

Quantum Monte Carlo Simulation of Exciton-Exciton Scattering in a GaAs/AlGaAs Quantum Well

J. Shumway¹

Dept. of Physics and Astronomy, Arizona State University, Tempe, AZ 85287-1504

Abstract

We present a computer simulation of exciton-exciton scattering in a quantum well. Specifically, we use quantum Monte Carlo techniques to study the bound and continuum states of two excitons in a 10 nm wide GaAs/Al_{0.3}Ga_{0.7}As quantum well. From these bound and continuum states we extract the momentum-dependent phase shifts for s-wave scattering. A surprising finding of this work is that a commonly studied effective-mass model for excitons in a 10 nm quantum well actually supports two bound biexciton states. The second, weakly bound state may dramatically enhance exciton-exciton interactions. We also fit our results to a hard-disk model and indicate directions for future work.

Key words: Excitons, Quantum wells, Quantum Monte Carlo, Scattering
PACS: 78.67De, 02.70.Ss, 71.35Ay

1. Introduction

Exciton-exciton interactions in quantum wells are becoming increasingly important to science and technology. For example, the interaction of two excitons is a mechanism for non-linear optical response [1]. It is the excitonic component of polaritons that lead to their interactions. Also, in experimental studies of cold excitonic gases in quantum wells, exciton-exciton scattering is a process that drives the excitons towards a Bose distribution.

Exciton-exciton interactions are difficult to theoretically predict [2]. Fast collisions between excitons may be treated with time dependent perturbation theory [3]. Carrier exchange is known to be a significant contribution to the scattering process [3]. At a different

extreme, slow moving excitons interact through dipole interactions. If the excitons have intrinsic dipoles, perhaps from carefully engineered quantum well band-structure or an applied electric field, the repulsive dipole-dipole force can dominate interactions [1,4]. In the more common case of unpolarized excitons, quantum fluctuations of the polarization leads to attractive van der Waals interactions, which are often neglected. Finally, we know that the wavefunction describing elastic exciton collisions must be orthogonal to any bound biexciton states. The presence of weakly bound biexciton states can have dramatic effect on exciton scattering cross-sections [2].

In this work we have extended a quantum Monte Carlo technique in order to study exciton scattering in a GaAs/Al_{0.3}Ga_{0.7}As quantum wells. An earlier paper studied bulk exciton-exciton scattering for a generic model of a semiconductor [2]. The simula-

¹ Email: shumway@mailaps.org

tion technique directly samples the energy of the four-particle scattering wavefunction. This allows all mechanisms listed in the previous paragraph — carrier exchange, dipole and van der Waals forces, and orthogonality to bound biexcitons — to be fully incorporated in the numerical simulation. Random walks are used to project essentially exact energies from a set of trial wavefunctions, thus providing numerical estimates of the phase shifts and scattering cross sections for elastic exciton-exciton collisions. Our new calculations apply this technique to a quantum well, allowing a detailed study of the exciton-exciton collision process within the effective mass approximation. Two key results of these calculations are the observation of a second, weakly-bound biexciton and the numerical estimate of a large cross-section ~ 100 nm for low-energy exciton-exciton scattering in a quantum well.

In the next section of this paper, we describe the effective mass model we use. After that we give a brief description of our computational technique and details of our simulation of a GaAs/Al_{0.3}Ga_{0.7}As well. The last section is a discussion that emphasizes new results of this paper, some subtleties of two-dimensional scattering, and future directions for this research.

2. Model

We use a single-band effective mass model,

$$H = \frac{\hbar^2}{2m_e} (r_1^2 + r_2^2) + \frac{\hbar^2}{2m_h} (r_a^2 + r_b^2) + \frac{e^2}{r_{12}} + \frac{1}{r_{ab}} + \frac{1}{r_{1a}} + \frac{1}{r_{2b}} + \frac{1}{r_{1b}} + \frac{1}{r_{2a}} + V_e(z_1) + V_e(z_2) + V_h(z_a) + V_h(z_b) \quad (1)$$

Here the electrons are labeled 1 and 2 and the holes are labeled a and b. The isotropic effective masses are $m_e = 0.0667m_0$ and $m_h = 0.34m_0$, and the dielectric constant is $\epsilon = 12$. (Future calculations will include the anisotropy of the heavy-hole mass.) The confining potentials V_e and V_h are finite square wells with depths $V_e = 216$ eV and $V_h = 133$ meV. These material constants have been chosen to match other theoretical studies of excitons and biexcitons in GaAs/Al_{0.3}Ga_{0.7}As quantum wells for direct comparison with this work [5,6].

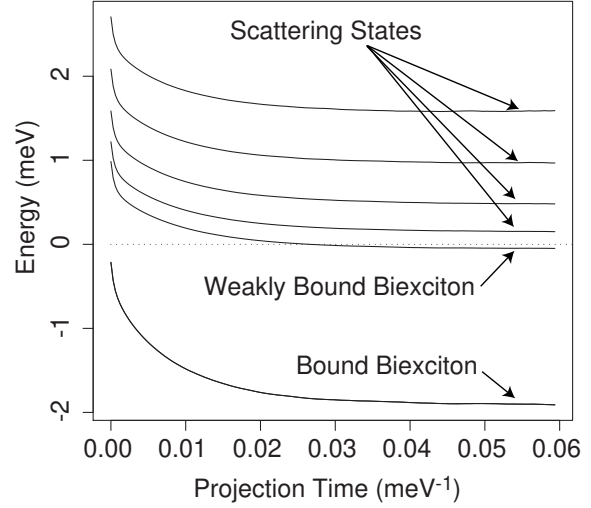


Fig. 1. Projection of eigenvalues with a random walk in imaginary time (shown for the simulation with $r_{\text{cut}} = 180$ nm). The projection over an imaginary time 0.06 meV^{-1} takes a buffer of 200 Monte Carlo steps.

The electron effective mass and dielectric constant define natural length and energy scales for the problem: the donor effective Bohr radius, $a_B = \hbar^2 / m_e e^2 = 9.97$ nm, and the donor effective Rydberg, $R_{\text{yd}} = \sim 2m_e a_B = 5.79$ meV. In this paper we present numerical answers to three digits for comparison to other theoretical papers; such accuracy is beyond the limits of the effective mass model and the leading digit should suffice for comparison to experiments.

For a well of width 9.97 nm, we find an exciton binding energy of 9.22 meV, using QMC methods described in the next section. Previously published QMC calculations report energies of about 10.0 meV for the exciton binding energy at this well width [5,6]. We have also calculated the biexciton binding energy, which is around 1.87 ± 0.01 meV, in very good agreement with experimental [7] and theoretical [8] values.

We also see a second, very weakly-bound excited biexciton state with binding energy 0.032 ± 0.007 meV. This state is not likely to be directly observable, but it can have a big influence on the scattering length. Also, note that this calculation is within the effective-mass approximation with isotropic effective masses, and the bound state may be an artifact of this approximation. Nevertheless, this result suggests that a second bound biexciton state is possible in a GaAs/AlGaAs quantum well.

3. Calculation Technique and Results

We use random walks to project a set of wavefunctions in imaginary time, as described in Ref. [2]. We first construct variational wavefunctions corresponding to a bound state and excited state of scattering. The excitons can be paired two ways: electron 1 can be paired with hole a and electron 1 with hole b, which we denote $1a;2b$, or we can have the pairing $1b;2a$. Eigenstates are symmetric or antisymmetric combinations,

$$= \frac{1}{\sqrt{2}} (|1a;2b\rangle \pm |1b;2a\rangle) \quad (2)$$

These wavefunctions can be related to spin states through the symmetry of the wavefunction. In these calculations we are just studying the $++$ wavefunction, since this is the one that has the bound biexciton. This is one channel for scattering, and to get cross sections for different exciton spin states we will need to study $+-$ also.

Next we discretize the scattering states by restricting the excitons to never be separated by a distance greater than R_n . We choose values of R_n between 160 nm and 280 nm. This turns the scattering states into standing waves we can study with QMC. Using QMC, we project the wavefunction with a random walk. The random walk is repeated projection of the wavefunction with $\exp(-H\tau)$. In Fig. 1 we show the projection of eigenvalues from the simulation with $R_n = 200$ nm. We clearly see the bound biexciton projected to an energy of about -1.9 meV. There is also a much more subtle feature: a second weakly bound biexciton state. This can be thought of as a quantized vibrational excitation in the radial exciton-exciton separation coordinate.

In Fig. 2 we show the energy eigenvalues for a series of different R_n values. We see that the two bound states are relatively insensitive to the boundary condition, while the scattering states systematically decrease in energy with increasing R_n . These energy curves hold all the information about low energy s-wave scattering.

Since we know the energies of the scattering states, we know the relative momentum k . Because we know the scattering function has a node at R_n , we can infer the phase shift, $\delta(k)$. We plot the phase shift in Fig. 3. Again, the weakly bound vibrationally excited biexciton shows up, this time as the phase tends to 2π , indicating two bound states. The scatter in this data is the Monte Carlo noise from our simulations.

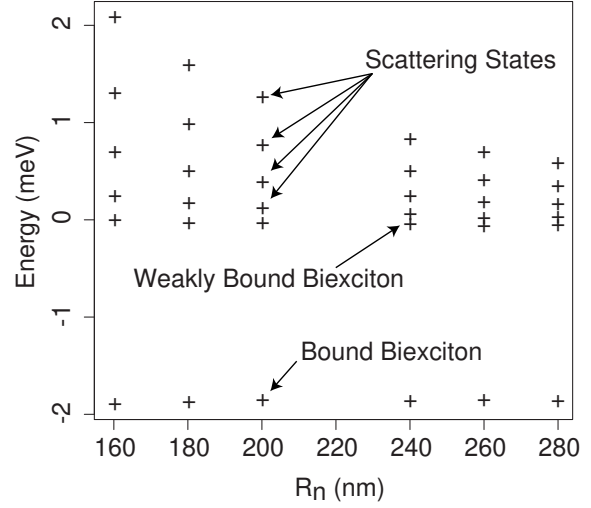


Fig. 2. Energy vs. cutoff. Small, random fluctuations are the statistical noise in the Monte Carlo simulations.

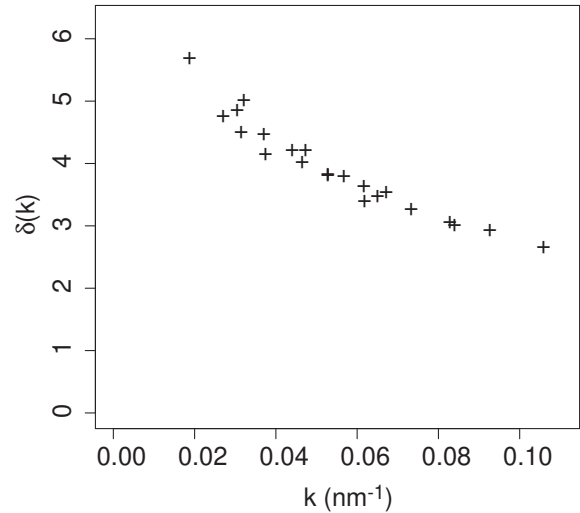


Fig. 3. Phase shifts calculated from data points in Fig. 2.

From the phase shift, we calculate the s-wave scattering cross sections, given by $\sigma = 4 \sin^2(\delta(k))/k$. Fig. 4 shows the scattering cross sections from our raw Monte Carlo data. At low energy, the cross section becomes quite large, ~ 100 nm. Two effects may contribute: (1) the weakly-bound excited biexciton state at 0.03 meV can enhance scattering, and (2) two dimensional systems have a logarithmic divergence of the scattering cross-section at low energy. The statistical error in these simulations prevents us from distinguishing be-

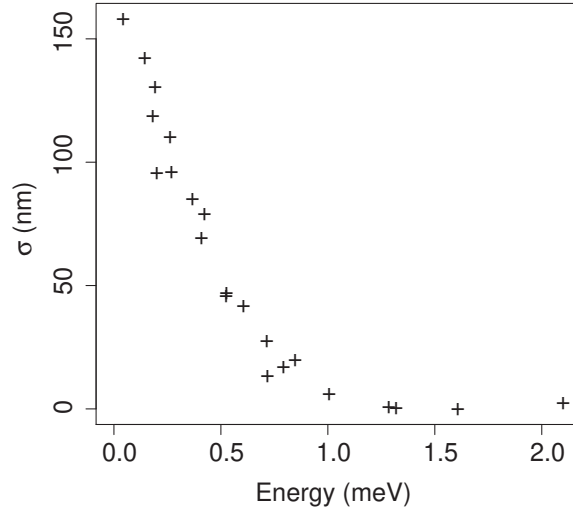


Fig. 4. Two-dimensional scattering cross sections (with dimension of length) from data points in Fig. 3.

tween these contributions.

4. Discussion

Scattering in two dimensions differs significantly from three-dimensional scattering [9]. In particular, the scattering length can no longer be simply obtained from an effective range expansion [10]. In three dimensions, the scattering length characterizes the interaction strength for low energy collisions. The corresponding quantity in two dimensions is dimensionless: the scattering is characterized by an effective range and a dimensionless parameter. As a simple analysis, we will extract just one parameter from our results by fitting our phase shifts to a hard-disk model. This analysis cannot capture resonant effects from the weakly bound state, but it does provide a useful length scale.

The phase shift for s-wave scattering for hard disks of radius a in two dimensions is

$$\frac{\gamma}{2} \cot \gamma = \ln \frac{ka}{2} + \frac{1}{4} a^2 k^2 + O(k^4); \quad (3)$$

where $\gamma = 0.5772:::$ is the Euler-Mascheroni constant. A crude fit of our calculated values of $\frac{\gamma}{2} \cot \gamma$ to the hard disk formula gives $d = 2.8a_B$ with a statistical uncertainty of about 10%. This suggests the excitons can be approximated as hard disks with radii of 27 nm,

if the electron and hole spins are each in singlets as required by our $++$ wavefunction.

Now we must consider spin. We have only simulated the $++$ scattering states. In bulk, three-dimensional calculations, the $++$ have a much smaller contribution to the scattering, since there is now bound biexciton when electrons and holes are spin polarized [2]. Using Table III of Ref. [2] and neglecting the $++$ contribution, we approximate the scattering cross section of paraexcitons as $\frac{1}{16}$ the symmetric value, or 1.7 nm. Two orthoexcitons in a relative $S = 0$ state have a scattering cross section that is $\frac{1}{2}$ the symmetric value, or 13.5 nm. Recall that this hard disk analysis neglects resonant effects from the weakly bound excited biexciton.

Future work will include a study of $++$ and scattering channels for different geometries. We will also attempt to extract two parameters, an effective range and a scattering strength, from our calculations. Such a parameterization could provide input for models of thermal equilibration rates and properties a weakly-interacting Bose condensate of excitons.

References

- [1] T. Hiroshima, E. Hanamura, M. Yamashita, Phys. Rev. B 38 (1988) 1241{1245.
- [2] J. Shumway, D. M. Ceperley, Phys. Rev. B 63 (2001) 165209.
- [3] C. Cui, V. Savona, C. Piermarocchi, A. Quattropani, Phys. Rev. B 58 (1998) 7926{7933.
- [4] T. S. Koh, Y. P. Feng, H. N. Spector, J. Phys.: Condens. Matter 9 (1997) 7845{7853.
- [5] C. Riva, F. M. Peeters, K. Varga, Phys. Rev. B 61 (2000) 13873{13881.
- [6] A. V. Filinov, M. Bonitz, Y. E. Lozovik, Phys. Stat. Sol. (c) 0 (2003) 1441{1444.
- [7] S. Adachi, T. Miyashita, S. Takeyama, Y. Takagi, A. Tackeuchi, M. Nakayama, Phys. Rev. B 55 (1997) 1654{1660.
- [8] T. Tsuchiya, Phys. Stat. Sol. (c) 1 (2004) 603{607.
- [9] S. K. Adhikari, Am. J. Phys. (1986) 362{367.
- [10] S. K. Adhikari, W. G. G. T. K. Lim, J. Chem. Phys. 85 (1986) 5580{5583.